

Electronic Supporting Information

## Robust Monolithic Metal-Organic Framework with Hierarchical Porosity

Sérgio M. F. Vilela,<sup>1§</sup> Pablo Salcedo-Abraira,<sup>1§</sup> Loïc Micheron,<sup>2</sup> Eugenio L. Solla,<sup>3</sup> Pascal G. Yot,<sup>4</sup> and Patricia Horcajada<sup>1,2\*</sup>

<sup>1</sup> Advanced Porous Materials Unit (APMU), IMDEA Energy Institute, Avda. Ramón de la Sagra 3, E-28938 Móstoles, Madrid (Spain); E-mail: [patricia.horcajada@imdea.org](mailto:patricia.horcajada@imdea.org); Tel: +34 917371120

<sup>2</sup> Institut Lavoisier de Versailles, Université de Versailles St Quentin, UMR CNRS 8180, 45 avenue des Etats-Unis, 78035 Versailles, University Paris Saclay, France

<sup>3</sup> Servicio de Microscopía Electrónica, CACTI, Universidade de Vigo, Campus Lagoas Marcosende, 36310 Vigo, Pontevedra, Spain

<sup>4</sup> Institut Charles Gerhardt Montpellier, UMR 5253, CC15005, Université de Montpellier, Place Eugène Bataillon, 34095 Montpellier Cedex 05, France

§ Equally contributing authors

## General Instrumentation

X-ray powder diffraction (XRPD) patterns were collected in a D8 Advance Bruker diffractometer with Cu K $\alpha$ 1 radiation ( $\lambda = 1.54056 \text{ \AA}$ ) from 3 to 35° (2 $\theta$ ) using a step size of 0.02° and 2.5 s per step in continuous mode.

Transmission electron microscopy (TEM) images were acquired in a Darwin 208 Philips microscope (60-80-100 KV; Camera AMT).

Fourier Transform infrared (FTIR) spectra were recorded in a Thermo Nicolet spectrometer (Thermo, USA) from 4000-400 cm<sup>-1</sup>.

Thermogravimetric analyses (TGA) of the nano-sized UiO-66-NH<sub>2</sub> (5-10 mg) were performed using a Perkin Elmer Diamond TGA/DTA STA 6000 (Connecticut, USA) under air flow (20 mL min<sup>-1</sup>) running from room temperature to 600 °C with a heating rate of 3 °C min<sup>-1</sup>.

N<sub>2</sub> sorption measurements were carried out at 77 K on a Belsorp Max<sup>®</sup> porosimeter (BEL Japan Inc.). Prior to the measurements, samples were degassed under secondary vacuum and heated at 160 °C for 3 h.

The particle size and zeta potential were measured using a Malvern Instruments Zetasizer Nano series Nano-ZS<sup>®</sup>. The nanoparticles were dispersed using a Branson Digital Sonifier<sup>®</sup> (Connecticut, USA, 400 W) at 10% of amplitude for 1 minute.

## Reagents and Solvents

2-Aminoterephthalic acid (Acros Organics, 99%), *N,N'*-dimethylformamide (DMF, ChemLab, 99.5%), ZrOCl<sub>2</sub>·8H<sub>2</sub>O (Sigma-Aldrich, 99.5%), ethanol (absolute, J.T. Baker). All reagents and solvents were used as received for the commercial suppliers without further purification.

## Synthesis of UiO-66-NH<sub>2</sub> Nanoparticles

2-Aminoterephthalic acid (0.0906 g) was dissolved in DMF (5 mL) and ZrOCl<sub>2</sub>·8H<sub>2</sub>O (0.1612 g) was then added. The resulting reactive mixture was stirred at 90 °C for 4 h and, then, immediately cooling down in an ice bath. The solid was collected by centrifugation (13,000 rpm for 15 min), suspended in DMF, dispersed in an ultrasound bath (for approximately 30 s) and recovered by centrifugation (13,000 rpm for 15 min). Finally, the solid was washed with ethanol by dispersing in an ultrasound bath and recovered by centrifugation (13,000 rpm for 15 min). The last step was repeated for six times for a complete activation. Yield: 73%.

## Shaping of UiO-66-NH<sub>2</sub> Nanoparticles

UiO-66-NH<sub>2</sub>-based monoliths were prepared by using two distinct protocols:

*i)* 0.7 cm-diameter plastic tube up to 1-2 cm-height were filled with ethanolic solutions of UiO-66-NH<sub>2</sub> nanoparticles (NPs) at different concentrations (10, 20 and 55 mg mL<sup>-1</sup>). Plastic tubes were transferred into a desiccator provided with silica gel and kept until their fully drying (2, 7 and 9 days for the concentrated solutions of 10, 20 and 55 mg mL<sup>-1</sup>, respectively; Fig. S5).

*ii)* Before drying under supercritical CO<sub>2</sub>, UiO-66-NH<sub>2</sub> NPs were washed with pure ethanol (absolute 200 proof Molecular Biology Grade, Fisher Bioreagents). Then, the corresponding ethanolic solutions of the MOF, with the same concentrations of those mentioned in *i)*, were introduced in a 0.7 mm-diameter plastic tube up to 1-2 cm-height. A typical supercritical CO<sub>2</sub> activation process was performed using a TOUSIMIS Samdri-PVT-3D instrument. The plastic tube containing the gel was loaded into a glass cell and transferred to the instrument chamber. After cooling the chamber at 0-10 °C, the cell was filled with liquid CO<sub>2</sub> followed by 5 min of purge. The gel was soaked in liquid CO<sub>2</sub> for 25 min, keeping the temperature between 0 and 10 °C. The purge-

soaking cycle was repeated 9 times. Then, a last cycle was carried out and the temperature was turned on supercritical temperature (40-42 °C) for 2 h. After reaching supercritical temperature and pressure ( $\approx 800$  psi), the system was allowed to slowly breed overnight, collecting then the resulting monolith.

Before transferred to the supercritical CO<sub>2</sub> equipment, the 20 mg mL<sup>-1</sup> ethanolic solutions were firstly kept for 1 day in a desiccator provided with silica gel. After that, the protocol toward the preparation of 20 mg·mL<sup>-1</sup> SiO<sub>2</sub>/1d SC monolithic pieces is the same than that described in the last paragraph.

### **Mercury Intrusion Porosimetry (MIP)**

MIP experiments were carried out in UiO-66-NH<sub>2</sub> NPs-based monoliths using a Hg porosimeter Micromeritics Autopore 9240 at room temperature. Density and particle size distribution were determined in the 0.1-413 MPa pressure range. All the samples were preliminary outgassed during 15 min to reach a pressure of  $\approx 6.5$  Pa before the collection. Mercury intrusion curves (Fig. S11) allowed the determination of the density of the powdered materials and estimation of the pore size distribution using Mayer and Stowe's method.<sup>1</sup>

The densities of the powdered monoliths were determined from the mercury intrusion using 13.534(1) g mL<sup>-1</sup> for the density of mercury. Two average particle diameters were found to be close of  $D_{p1} = 1200$  nm and  $D_{p2} = 3300$  nm. The mercury surface tension  $\gamma$  was taken as 0.485 N m<sup>-1</sup>, and the dimensionless Mayer-Stowe constant  $\kappa$ , was taken as 10.<sup>2,3</sup>

### **FIB-SEM Nanotomography**

FIB-SEM slice & view experiments were carried out with a Dual Beam FEI Helios Nanolab 600. FIB milling with Ga<sup>+</sup> ions was performed at a current of 0.28 nA at 30 kV, keeping a distance of 20 nm between consecutive slices. SEM images were acquired with a 5 kV beam at a working distance of 4 mm.

The obtained image stack was subsequently aligned and processed with FEI Amira Resolve RT in order to produce a 1.30 x 1.08 x 2.88  $\mu$ m 3D model of the porous MOF. Once the 3D model was obtained, it allowed performing further calculations to gather a deeper insight of the material. Therefore, a pore size distribution calculation was performed on FIJI<sup>4</sup> using the plugin developed by Münch *et al.*<sup>5</sup>

## Characterisation

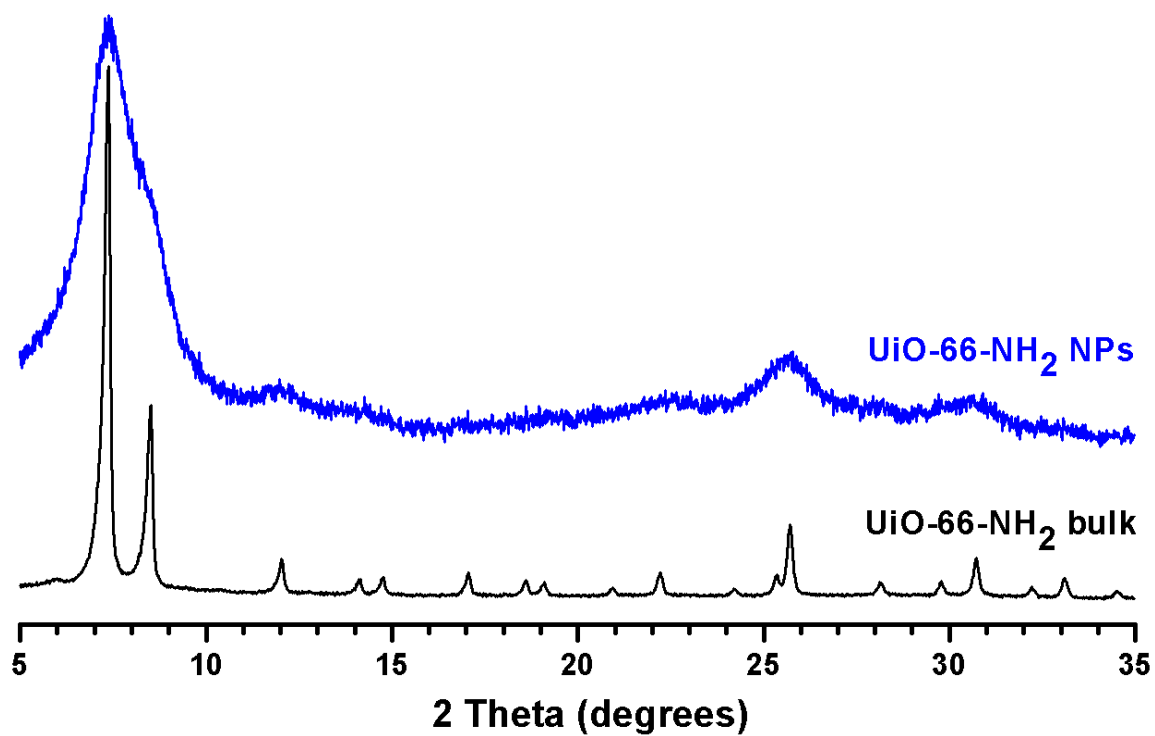


Fig. S1 PXRD patterns of the bulk (**black**) and nano-sized (**blue**) UiO-66-NH<sub>2</sub>.

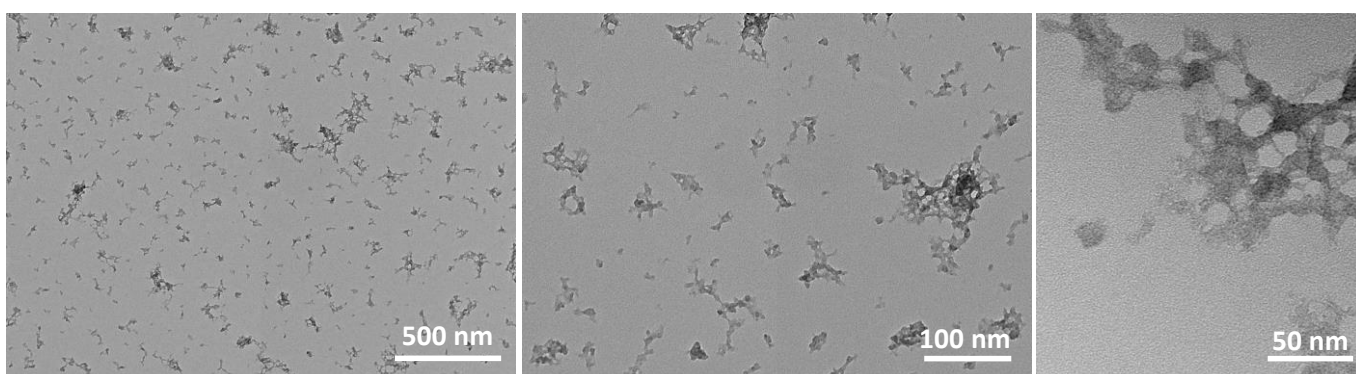
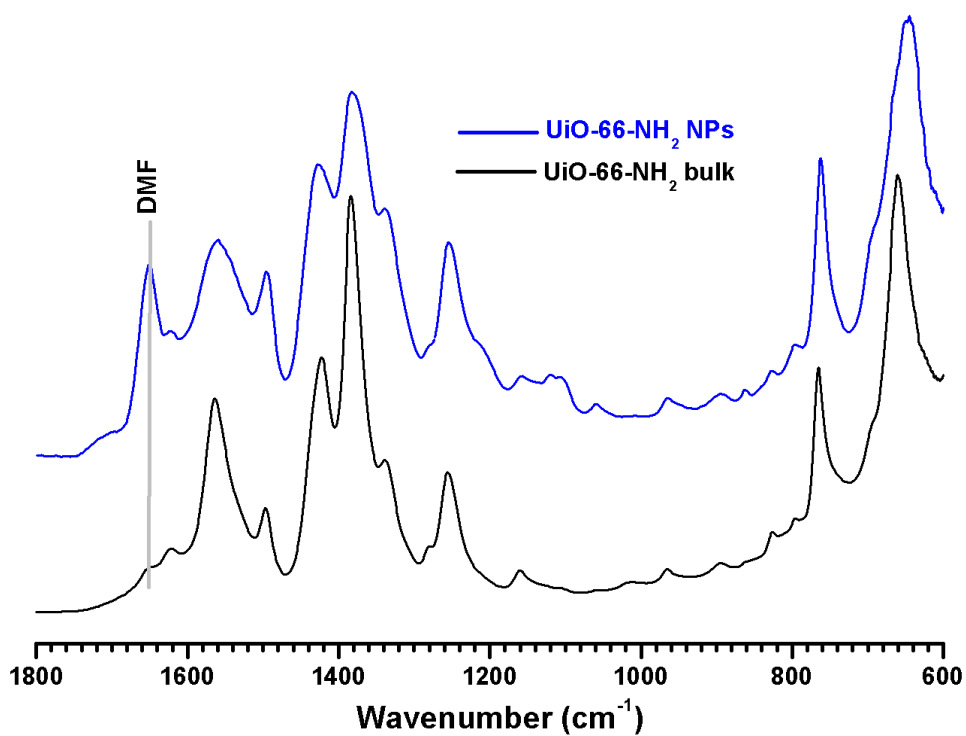
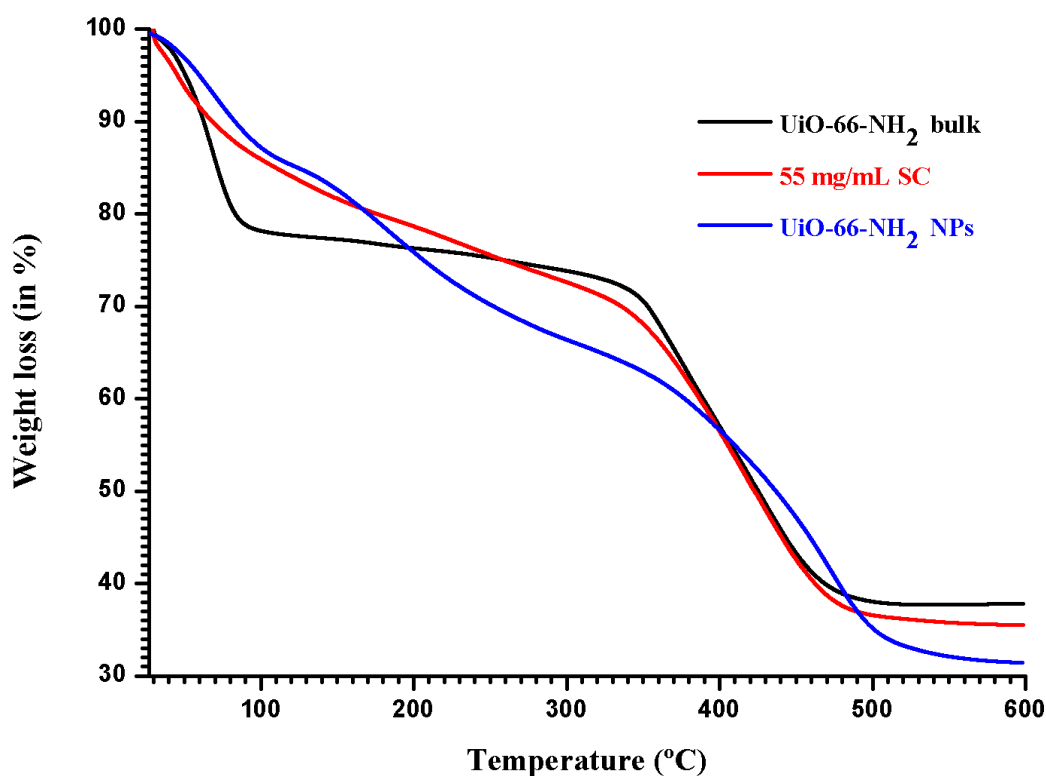


Fig. S2 TEM images of the activated UiO-66-NH<sub>2</sub> NPs.



**Fig. S3** Selected FTIR spectral range of the bulk (**black**) and nano-sized (**blue**) UiO-66-NH<sub>2</sub>. Both spectra are quite similar with variations in the intensity of some vibration bands. Nevertheless, the higher intensity of the 1652 cm<sup>-1</sup> band in the spectrum of UiO-66-NH<sub>2</sub> NPs corresponds to some residual DMF molecules, which were not completely removed from the NPs after the washing step.



**Fig. S4** TGA curves of the bulk (black) and UiO-66-NH<sub>2</sub> NPs (blue), and 55 mg·mL<sup>-1</sup> SC monoliths (red), confirming the chemical composition of the dried form of UiO-66-NH<sub>2</sub>, Zr<sub>6</sub>O<sub>4</sub>(OH)<sub>4</sub>[C<sub>8</sub>O<sub>4</sub>NH<sub>5</sub>]<sub>6</sub>, (ZrO<sub>2</sub> (theo. vs exp.) = 45.8 vs. 46.8%). An additional progressive weight loss between 150 and 250°C might correspond to some residual DMF, as confirmed by FTIR spectroscopy (Fig. S3). Although washed several times with ethanol, DMF was not completely removed from the pores of the NPs.

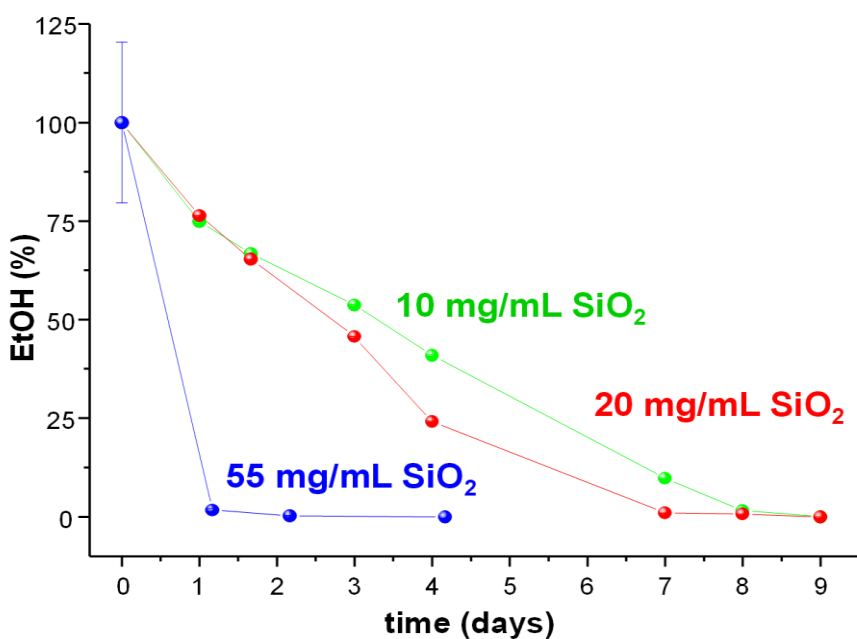


**Fig. S5** Drying process evolution of UiO-66-NH<sub>2</sub> NPs as a function of the concentration.

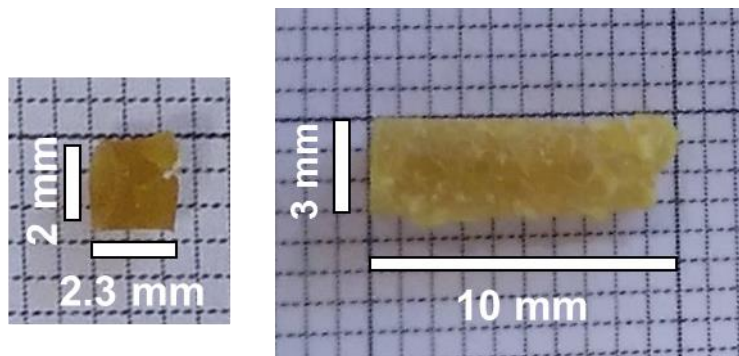


**Fig. S6**  $20 \text{ mg}\cdot\text{mL}^{-1} \text{ SiO}_2$  (*left*) and  $55 \text{ mg}\cdot\text{mL}^{-1} \text{ SiO}_2$  (*right*) monolithic pieces dried in a desiccator provided with silica gel for 7 and 1 days, respectively.

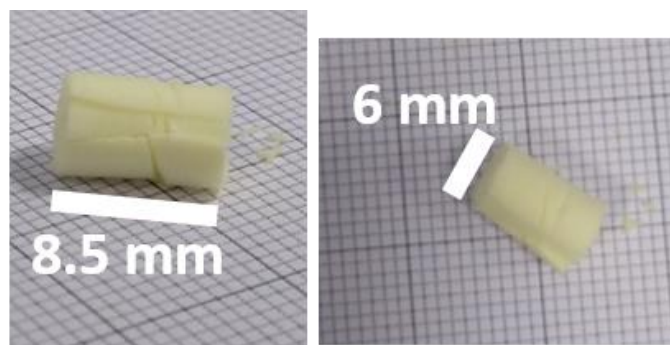


**Fig. S7** Pictures of a  $20 \text{ mg}\cdot\text{mL}^{-1} \text{ SC}$  monolith with some fractures, leading to its disintegration when pressed with 0.5 MPa.

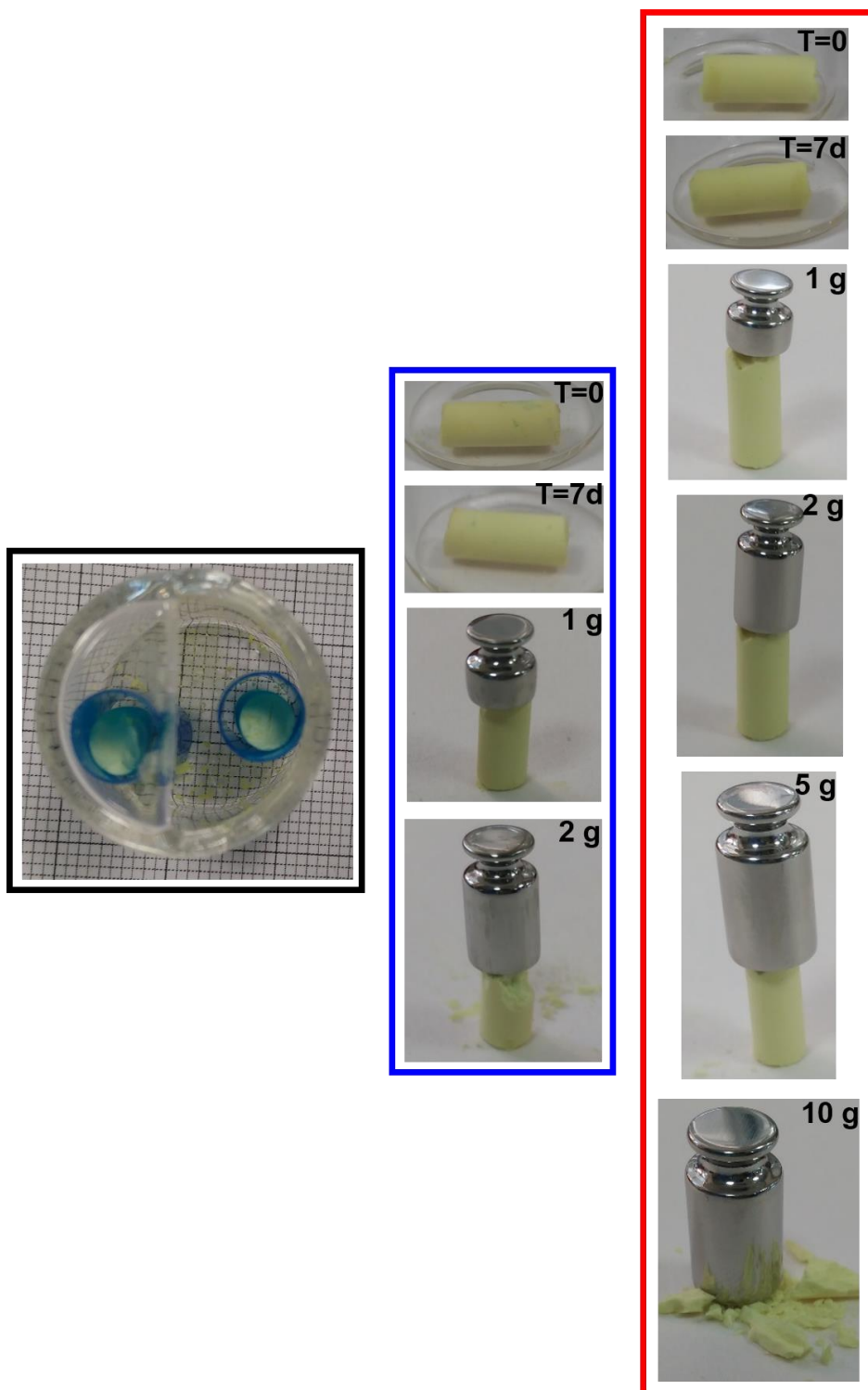


**Fig. S8** Pictures of two  $55 \text{ mg}\cdot\text{mL}^{-1}$  SC monoliths. **Black box:** monoliths inside of the plastic moulds and supercritical  $\text{CO}_2$  holder after drying. **Blue box:** T=0 – immediately after drying under supercritical  $\text{CO}_2$ ; T=7d – stored at atmosphere conditions for 7 days; 1 g – applying a weight of 1 g after 7 days; 2 g – applying a weight of 2 g after 7 days, leading to its disintegration. **Red box:** T=0 – immediately after drying under supercritical  $\text{CO}_2$ ; T=7d – stored under vacuum for 7 days; 1 g – applying a weight of 1 g after 7 days; 2 g – applying a weight of 2 g after 7 days; 5 g – applying a weight of 5 g after 7 days; 10 g – applying a weight of 10 g after 7 days, leading to its disintegration.

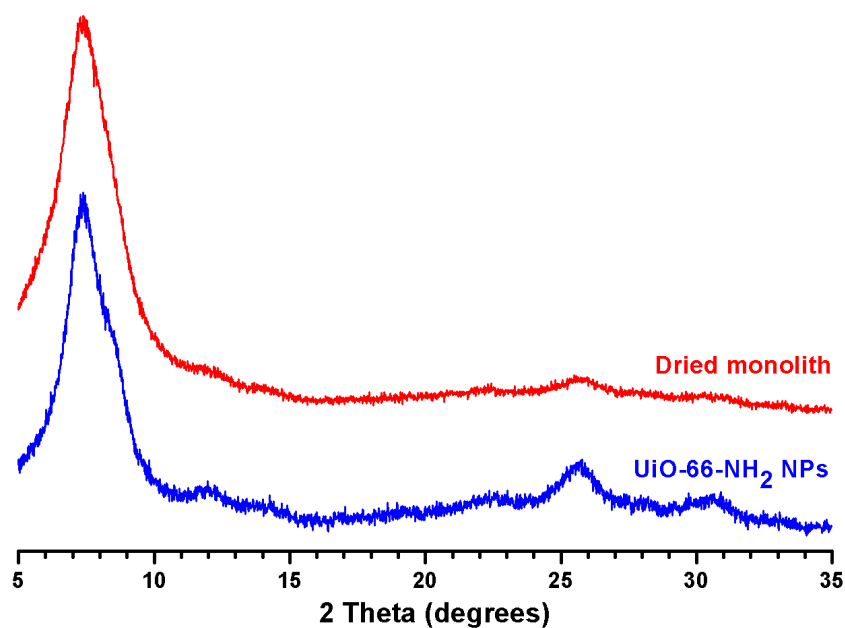


Fig. S9 PXRD patterns of UiO-66-NH<sub>2</sub> NPs (blue) and 55 mg·mL<sup>-1</sup> SC (red).

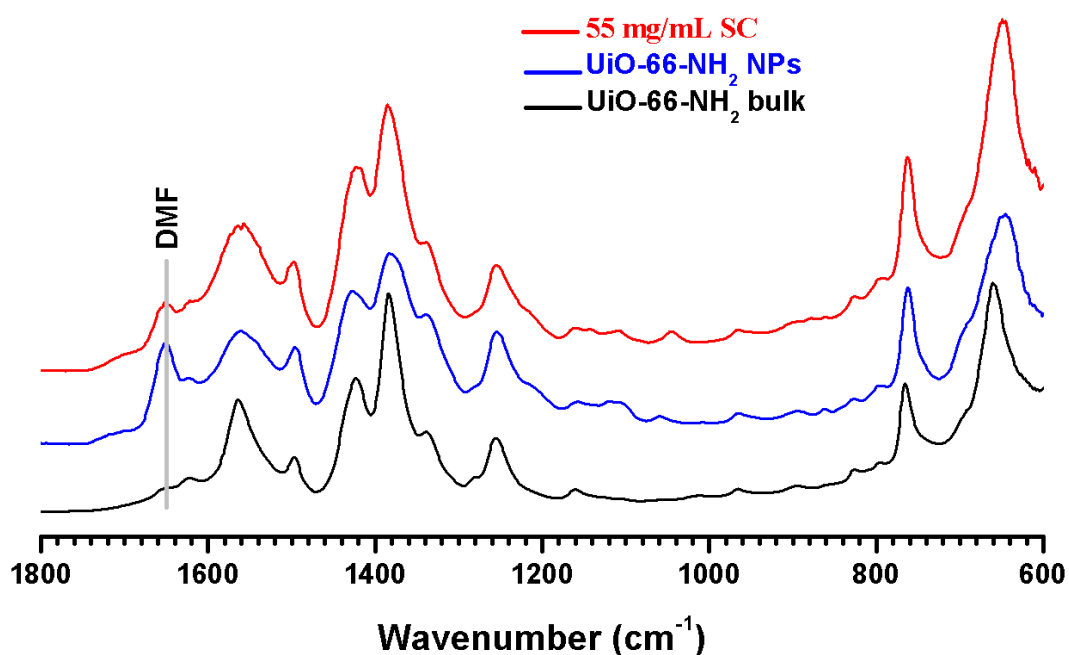
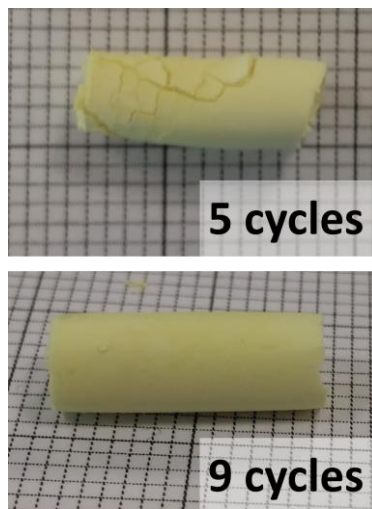
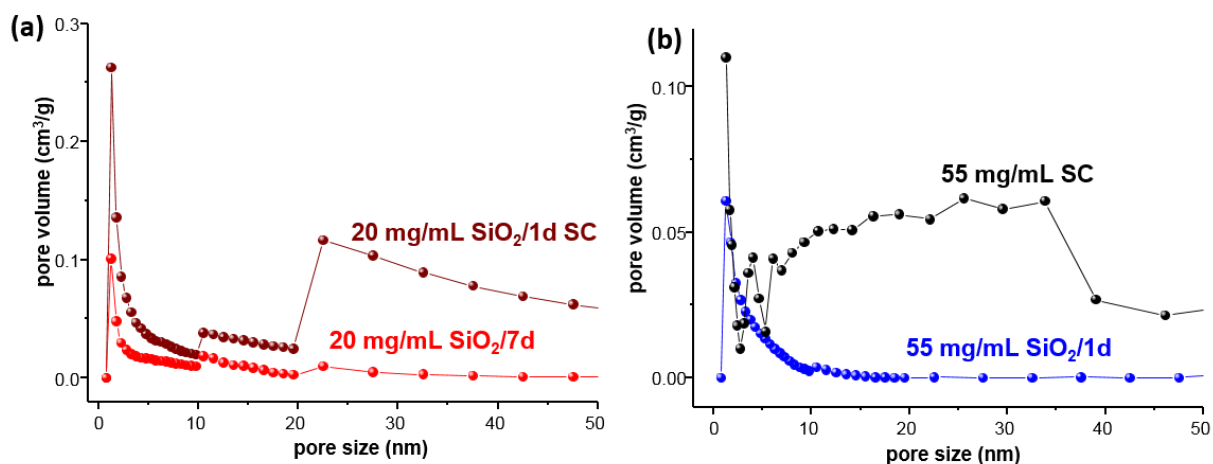


Fig. S10 Selected FTIR spectral range of the bulk (black) and nano-sized UiO-66-NH<sub>2</sub> (blue), and 55 mg·mL<sup>-1</sup> SC (red). As aforementioned, it is quite difficult to remove DMF molecules, even drying the monolith under supercritical CO<sub>2</sub>. Owing that, vibration modes peaking at *ca.* 1652 cm<sup>-1</sup>, attributed to DMF, are observed in all the spectra, being less intense for the 55 mg·mL<sup>-1</sup> SC dried monolith and almost inexistent for the bulk material.



**Fig. S11**  $55 \text{ mg}\cdot\text{mL}^{-1}$  SC Monoliths prepared by employing 5 (top) and 9 cycles (bottom) of purge-soaking cycles.



**Fig. S12** Pore size distribution for monolith pieces, obtained from the  $\text{N}_2$  desorption branch using the Barrett-Joyner-Halenda (BJH) method, performed by using different drying procedures: (a)  $20 \text{ mg}\cdot\text{mL}^{-1}$   $\text{SiO}_2/1\text{d}$  SC monolith dried in a desiccator provided with silica gel for 7 days (**red**) and  $20 \text{ mg}\cdot\text{mL}^{-1}$   $\text{SiO}_2/7\text{d}$  monolith dried for 1 day in silica gel followed by supercritical  $\text{CO}_2$  treatment (**brown**); (b)  $55 \text{ mg}\cdot\text{mL}^{-1}$   $\text{SiO}_2/1\text{d}$  monolith dried in a desiccator provided with silica gel for 1 day (**blue**) and  $55 \text{ mg}\cdot\text{mL}^{-1}$  SC monolith dried under supercritical  $\text{CO}_2$  (**black**).

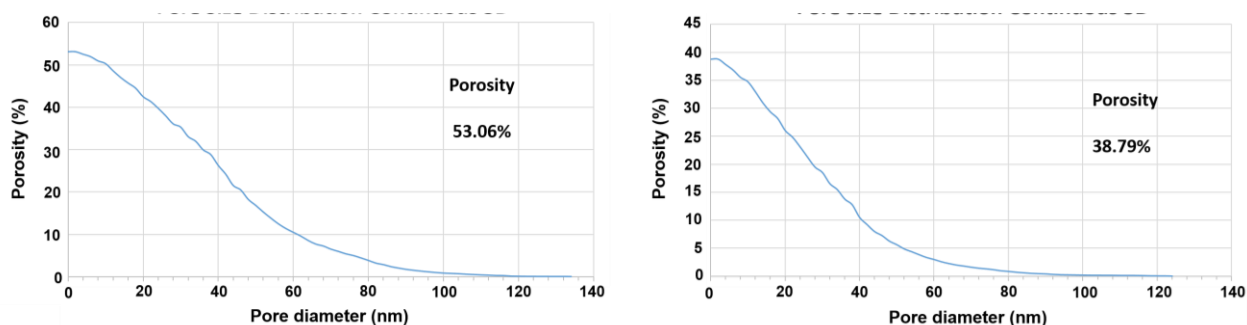


**Fig. S13** Pore size distribution calculated from FIB-SEM according to the methodology described in the experimental section for  $20 \text{ mg}\cdot\text{mL}^{-1} \text{ SiO}_2/1\text{d SC}$  (left) and  $55 \text{ mg}\cdot\text{mL}^{-1} \text{ SC}$  (right).

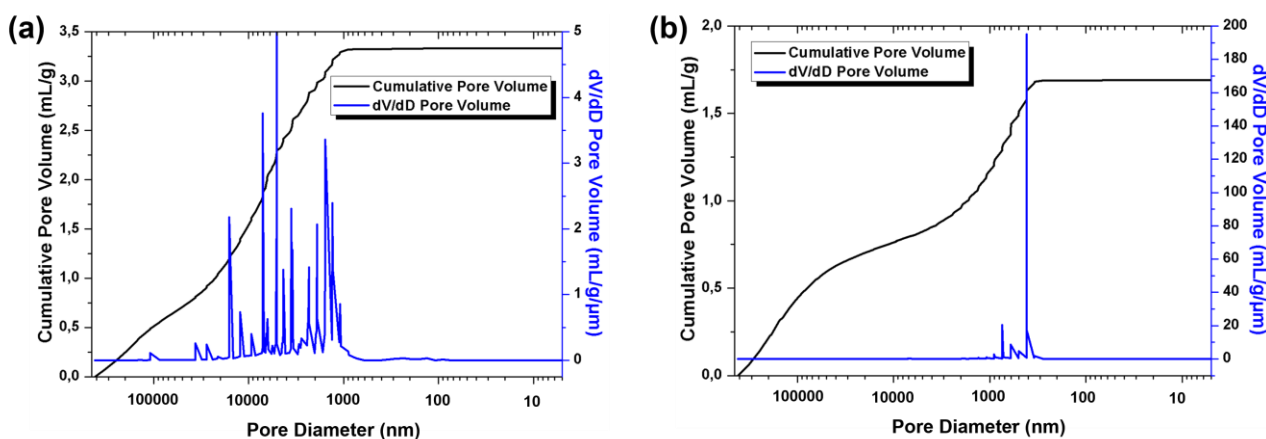


**Fig. S14** Pore size distribution and volume variation from MIP according to pore radius calculated on the 3D structure for the monoliths  $20 \text{ mg}\cdot\text{mL}^{-1} \text{ SiO}_2/1\text{d SC}$  (a) and  $55 \text{ mg}\cdot\text{mL}^{-1} \text{ SC}$  (b).

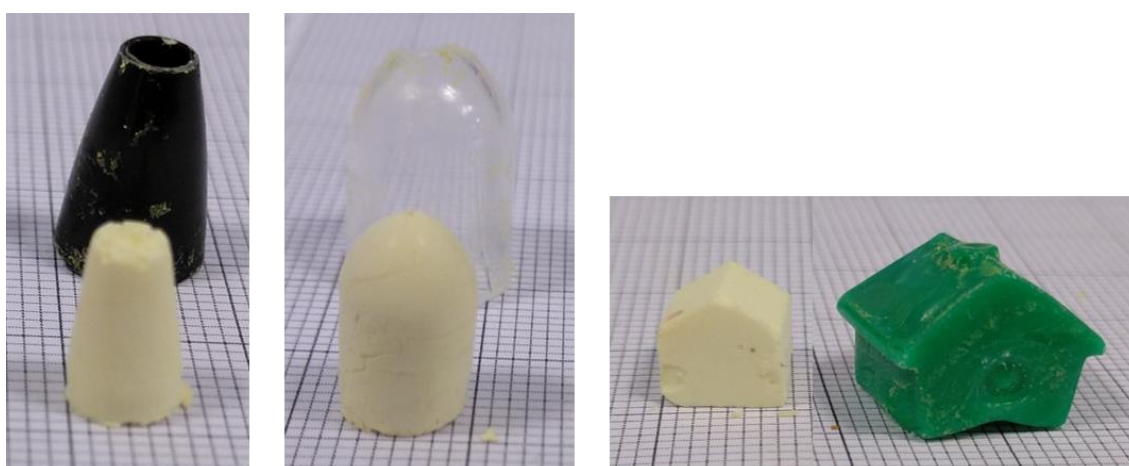


**Fig. S15** Images of  $55 \text{ mg}\cdot\text{mL}^{-1} \text{ SC}$  monoliths with different shapes: conical (left), round-top cylindrical (middle) and house-like (right) monolithic pieces.

**Table 1** Textural parameters for the dried monoliths 20 mg·mL<sup>-1</sup> SiO<sub>2</sub>/1d SC and 55 mg·mL<sup>-1</sup> SC.

Parameter	Technique	20 mg·mL <sup>-1</sup> SiO <sub>2</sub> /1d SC	55 mg·mL <sup>-1</sup> SC
Porosity (%)	FIB-SEM	53.1	38.8
	Hg intrusion	54.1	45.7
Bulk density (g·mL <sup>-1</sup> )	Hg intrusion	0.16	0.27
Apparent density (g·mL <sup>-1</sup> )	Hg intrusion	0.35	0.50
Total pore volume (mL·g <sup>-1</sup> )	Hg intrusion	3.3	1.7
Pore diameter (nm)	N <sub>2</sub> sorption.	5 - 40	25 - 100
	FIB-SEM	< 50	< 100
	Hg intrusion	1·10 <sup>3</sup> – 2·10 <sup>4</sup> > 2·10 <sup>4</sup> **	3·10 <sup>2</sup> – 3·10 <sup>3</sup> > 3·10 <sup>4</sup> **

\*\* These values are attributed to the cracks observed on Figs. 3f and g depicted in the main manuscript.

## References

- 1 R. P. Mayer and R. A. Stowe, *J. Colloid Sci.*, 1965, **20**, 893–911.
- 2 A. V. Neimark, F. X. Coudert, C. Triguero, A. Boutin, A. H. Fuchs, I. Beurroies and R. Denoyel, *Langmuir*, 2011, **27**, 4734–4741.
- 3 W. Pabst and E. Gregorova, in *ICT*, Prague, 2007.
- 4 J. Schindelin, I. Arganda-Carreras, E. Frise, V. Kaynig, M. Longair, T. Pietzsch, S. Preibisch, C. Rueden, S. Saalfeld, B. Schmid, J. Y. Tinevez, D. J. White, V. Hartenstein, K. Eliceiri, P. Tomancak and A. Cardona, *Nat. Methods*, 2012, **9**, 676–682.
- 5 B. Münch and L. Holzer, *J. Am. Ceram. Soc.*, 2008, **91**, 4059–4067.